Development of Empirical Vulnerability Curves for Electrical Supply Systems Subjected to Wind Hazard

Sarah Dunn
EPSRC Doctoral Prize Fellow, School of Civil Engineering and Geosciences, Newcastle University, Newcastle, UK

Sean Wilkinson
Senior Lecturer in Structural Engineering, School of Civil Engineering and Geosciences, Newcastle University, Newcastle, UK

Carmine Galasso
Lecturer in Catastrophe Risk Modelling, Dept. of Civil Engineering, Environmental and Geomatic Engineering and Institute for Risk and Disaster Reduction, University College London, London, UK

Lucy Manning
Research Associate, School of Civil Engineering and Geosciences, Newcastle University, Newcastle, UK

David Alderson
Research Assistant in GeoInformatics, School of Civil Engineering and Geosciences, Newcastle University, Newcastle, UK

ABSTRACT: In this paper, we develop a series of empirical vulnerability curves for energy distribution infrastructure in the UK, specifically for overhead line components, when subjected to wind storm hazard. We have achieved this by combining an atmospheric model, driven by reanalysis data, with empirical fault data from 1991 to 2010. The fault data used in this study comes from a national database of electricity distribution faults. While the fault data in this database is comprehensive, it has the deficiency of not recording the exact location of the fault, instead it only indicates which District Network Operator owned the asset. Better fault location information is available, but this is only available from the Operator. We also investigate the sensitivity of vulnerability curves to three different resolutions of the fault information; namely by Operator, Region and Area in order to evaluate the impact that this has to the vulnerability curve. From the results shown in this paper, we can conclude that the spatial resolution of the hazard data can have a significant impact to the vulnerability curve, particularly for large wind storm hazards.

1. INTRODUCTION

Fragility curves find their roots in earthquake engineering and, in simple terms, they describe how the structural performances – generally in terms of some limit state of interest – change over a range of loading conditions (i.e. the hazard intensity) to which that structure might be exposed (Schultz et al. 2010). Fragility curves were initially introduced and developed for conducting seismic risk assessments at nuclear power plants (Kennedy et al. 1980; Kaplan et al. 1983) and currently, the majority of publications developing (or using) fragility curves still appears to be in the area of seismic risk assessment, including studies by Basoz and Kiremidjian (1997) who developed fragility curves using observations of bridge damage following the Northridge earthquake that struck Los Angeles in 1994 and Lin (2008) who developed fragility

curves for frame structures when exposed to seismic loads. However, this method has also been applied to other hazards, including flooding and hurricanes; for example, Ellingwood et al (2004) developed fragility curves for lightweight wood frame structures to hurricane winds.

The development and application of fragility curves has traditionally focused on individual buildings or structures which have a static function; however, several recent research efforts are focusing on developing seismic fragility functions for the components of the global lifeline inventory (e.g., the Syner-G project; Pitilakis et al. 2014a-b). In fact, after a major disaster it is the functioning of the infrastructure systems which is of interest (i.e. the ability of a system to provide at least a baseline level of service), as these systems can either aid or hinder both short and long term recovery efforts. For example, the 2010 Haitian earthquake caused damage to the communication, transport and electrical systems which hampered rescue and aid efforts and led too many longer term problems, including the spread of disease.

In this paper, we develop empirically vulnerability curves for overhead line components of an electrical distribution system when subjected to wind storm hazard. These vulnerability curves plot the mean number of faults (or consumers involved) against wind speed and could be incorporated into future catastrophe risk models (e.g. Grossi and Kunreuther, 2005) to give an indication of the response of a system to an applied wind storm hazard. It should be noted that the vulnerability functions presented do not provide the probability of failure conditional on input intensity, but rather the average number of faults/consumers.

We have chosen to focus on wind storm hazards as this hazard has been shown to cause the highest number of faults to UK energy infrastructure (McColl et al. 2013). Fault data outlining the duration of the fault, number of consumers involved and the damaged component(s) for UK electrical distribution networks is recorded in the National Fault and Interruption Reporting Scheme (NaFIRS) database; however, this database does not record the intensity of the hazard which caused the fault (e.g. flood depth, wind speed) or the exact location of the fault. Therefore, we combine this fault data with wind hazard data which has been derived from a high resolution climate model, developed by the Dutch Meteorological Office, to empirically develop a range of vulnerability curves for different spatial resolutions as part of the ECLISE (Enabling Climate Information Services for Europe) project Wilkinson et al. (2014).

2. UK ENERGY DISTRIBUTION SYSTEMS

In the UK, transmission and distribution companies are responsible for transporting electrical power from generating plants to customers over their extensive networks. These systems are made up of many different types of equipment, including overhead lines, substations, cables and transformers, which all comply with British standards. The transmission system operates at typically 400kV or 275kV and the distribution system operates at voltages from 132kV to the normal household voltage of 230V (as shown in Figure 1). Distribution of power to customers is through a number of licensed geographically defined areas each controlled by a District Network Operator (DNO) and to give a sense of scale, in the UK there are over 800,000km of overhead and underground cables (PricewaterhouseCoopers LLP 2010).

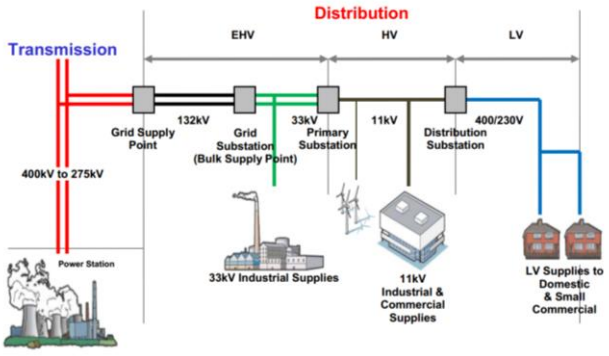

Figure 1: Typical Electricity Supply Chain (Energy Networks Association, 2011).

Weather related hazards have the potential to cause widespread disruption and interruptions to customer supplies. A study by the Met Office in 2008 showed that, from all weather-related events (including, rain, snow, lightning and flooding), wind storms cause the largest number of faults, in both the distribution and transmission systems (Met Office 2008). Their study also showed that the number of wind storm faults varies by region, with 56% of all faults in Scotland and Northern Ireland occurring due to wind and gale, falling to 50% for North England, the Midlands and North Wales and to 45% for South England and South Wales. Wind storms mainly cause disruption through damage to overhead power lines caused directly by the high wind speeds or more frequently, by windborne materials or falling trees and pose the greatest risk to the low voltage distribution network. Although this type of event can be disruptive to consumers, repairs can "*normally be carried out relatively quickly and typically most customers' supplies are usually restored within a few days*" (Energy Networks Association 2011). This type of extreme weather event is also highlighted in the 2013 National Risk Register to be one of the main risks which has the potential to affect the UK within the next five years (Cabinet Office 2013). This report gives storms and gales a relative likelihood of occurrence in the next five years between 1 in 200 and 1 in 20, the same as inland flooding and severe wildfires.

There are several events, most notably occurring in 1987, 1990, 1997, 1998 and 2002, which have highlighted the damage that wind storm events can have to energy infrastructure and also the impact that this damage can have to consumers. The 1987 storm was "*widely acknowledged to be Great Britain's most severe windstorm since 1703"* (Risk Management Solutions 2007) and exposed parts of the UK experienced wind speeds in excess of 110 mph. The storm left many hundreds of thousands of households without power, causing a total of 2.3 million power disconnection days (Gittus 2004). Power disruption was also experienced at Gatwick airport, causing a disruption to air travel. The storm was also notable for its effects to forests in the UK, causing the loss of 15 million trees (Risk Management Solutions 2007). As a result, much of the damage to property and infrastructure was attributed to falling trees and other windblown debris. Windstorm 'Kyrill' swept across Europe on 18th January 2007, causing damage across an area from Ireland to Poland. High wind speeds were recorded across the UK, with peak speeds of around 81mph (36.5m/s) in Blackpool, 73mps (33m/s) in Manchester and 67mps (30m/s) at Luton Airport (Willis Analytics 2007). Kyrill was reportedly the worst storm to hit the UK in 17 years, causing major disruption to infrastructure and power cuts to many households, including 100,000 in Surrey and 30,000 in Wales (Willis Analytics 2007).

3. WIND DATA

Hourly records of observed wind in the UK are recorded at a number of locations throughout Britain by the Met Office. These comprise both hourly mean wind and hourly maximum gust data, where the gust is averaged over a 3-second interval. However, not all of these records are simultaneous or continuous (there are often large periods of time with no data). There are also large areas of Britain which are not 'covered' by an observation station (e.g. the west of Scotland and the majority of Wales), as shown in Figure 2.

To produce a 'regular grid' of observational data over the UK this observational data has been used in 'reanalysis models', forming an 80km grid of surface gust speed, sea level pressure and wind speeds at the 850hPa pressure level at 6-hourly intervals (ERA-Interim data, Dee et al. 2011). However, this data is not of high enough resolution to give a likely failure wind speed for this method. Therefore, in this paper we use wind hazard data that has been derived from a high resolution atmospheric model. Wind velocities have been generated using a 12km grid atmospheric KNMI (Koninklijk Nederlands Meteorologisch Instituut, Dutch: Royal Netherlands Meteorological Institute) model that has been 'driven' at the boundary by the ERA-

Interim reanalysis data (at an 80km resolution). The location of data, for both the 12km KNMI model, 80km ERA-Interim data and observation stations are shown in Figure 2. This data is available at 6-hourly intervals and at a spatial resolution of 12km across the whole of the UK. Further information, regarding the development of this wind data is available at Wilkinson et al (2014).

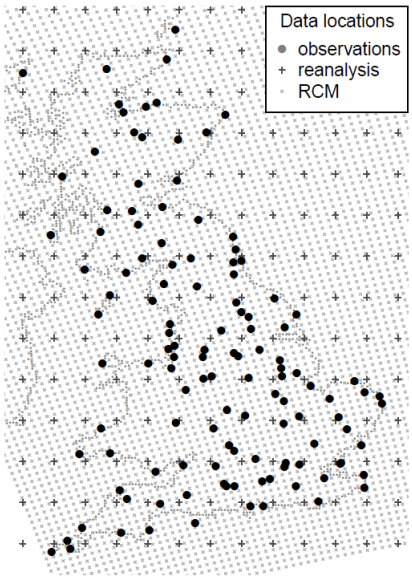

Figure 2: Showing the locations of data used (Wilkinson et al. (2014)).

4. VULNERABILITY CURVE METHODOLOGY

In this paper, we combine the information recorded in the NaFIRS database with the wind hazard data to form a series of vulnerability curves. As previously discussed, the wind hazard data records the maximum wind gust at 6-hourly intervals and therefore we assume that it is the nearest wind gust that caused the fault (as the NaFIRS database records the exact time of the fault, to the nearest minute). We 'count' the number of faults that occur within each 6-hourly interval and then plot the number of faults recorded in each of these time periods against the maximum wind speed recorded (and include all instances of zero faults on the plot). We also bin the wind data to the nearest integer to enable the average number of faults for each wind speed value to be calculated. This average is then plotted, for each integer value of wind speed, before fitting a trend line to obtain the shape of the vulnerability curve.

As previously discussed, the NaFIRS database does not record the exact location of the fault, but does record the DNO, Regions and Area in which the fault occurred. The relationship between these three spaces are shown in Figure 3 and to quantify the size of each, the DNO is approximately 60,000 km^2 (approximately 25% of the UK), the Region is approximately 15,000 km^2 and the Area is around 2,000 km^2. As we do not know the exact location of the fault, we develop three vulnerability curves to account for this lack of information. To do this, we assume that it is the maximum wind speed in each space at the time of the fault which caused the failure, with the Area wind speed being our benchmark (i.e. most precise information). This method also allows us to investigate the spatial sensitivity of our vulnerability curves, using the coefficient of variation.

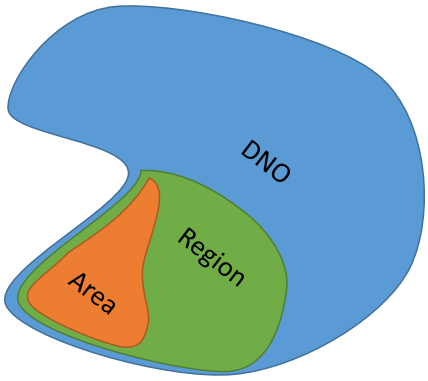

Figure 3: Showing the relationship between the whole of the District Network Operator (DNO), Region and Area spaces.

5. VULNERABILITY CURVE RESULTS AND DISCUSSION

The three vulnerability curves are plotted in Figure 4, in terms of both the mean number of faults recorded per 1000km and the proportion of consumers in the affected Area, for the maximum wind speed in the DNO, Region and Area. From this figure, it can be seen that overhead lines are

generally resilient, experiencing a very small number of faults (and consumers affected), when subjected to wind speeds of less than 20m/s, but increase in vulnerability, experiencing a greater number of faults, as this wind speed increases to more than 30m/s. It is worth noting that there are only a few instances of a wind speed over 30m/s being recorded, shown in Figure 5. From this figure, the differences in the wind speeds recorded between the DNO, Region and Area spaces can be seen. The DNO space records the highest wind speeds, reducing when the Region and Areas spaces are used. This indicates that the highest wind speeds in this DNO are not recorded in the Region or Area in which we are considering the faults. This figure also shows that the mode wind speed reduces as the size of the area considered reduces, from 15m/s for DNO to 12m/s for Region and 10m/s for Area.

Figure 4 also shows that vulnerability curves can be significantly affected by the spatial resolution of the wind data and that this also affects the scatter of the data. Figure 4(a) shows that there is a small amount of difference between the vulnerability curves calculated using the maximum wind speed in the DNO and Region, but that there is a significant difference when the maximum wind speed in the Area is used. This is particularly evident when considering faults which occur over 30m/s. For example, using the maximum wind speed in the Area records an average of 11 faults for a wind speed of 36m/s, however, this significantly reduces to 1.26 faults when the maximum wind speed in the DNO is used (a 158% difference). This is due to differences between the spatial location of the infrastructure and the location of the wind storm, as these high wind speeds may occur over sparsely populated, potentially mountainous areas, where there is little or no infrastructure. Therefore using either the larger scale DNO or Region wind speeds results in an overestimate of the failure the wind speed and an underestimation of the probability of failure of the component.

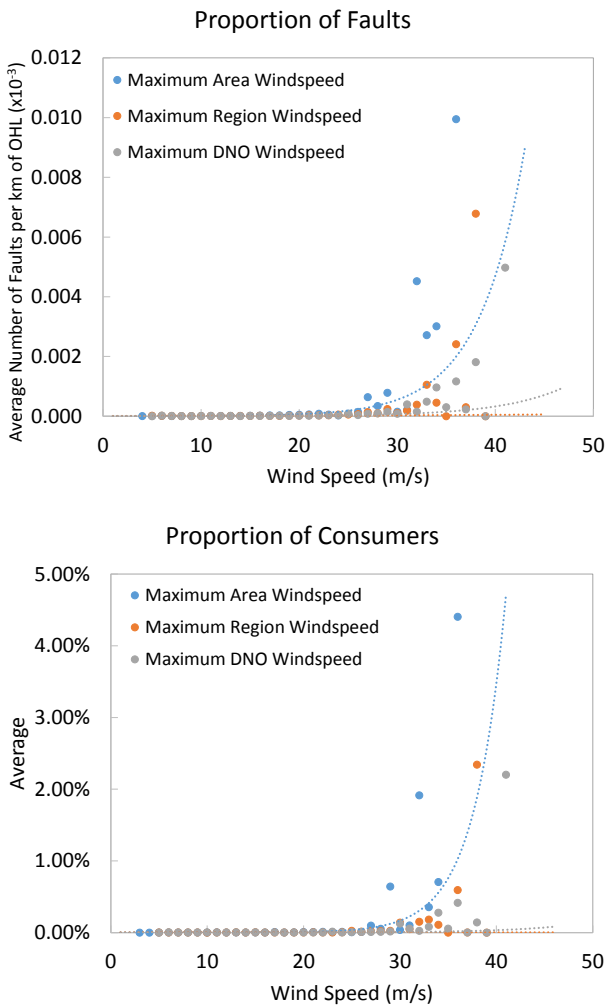

Figure 4: Plotting the mean proportion of (a) faults and (b) consumers affected as a proportion of the total number of consumers in the area, against maximum wind speed in the Area, Region and DNO space. In all cases the trend lines has been fitted using an exponential function. It is worth clarifying that whilst the data appears to show that there are more faults occurring within the Area space, the number of faults is constant throughout the whole analysis.

It is also worth noting that there are two points in the DNO and Region vulnerability curves that include zero faults for high values of wind speed (occurring at 35 and 39m/s). Again, these wind storms are likely to have occurred in regions where there is little or no infrastructure and further investigation of the data confirms this.

The spatial resolution of the wind data also affects the vulnerability curve when plotted in

terms of the proportion of consumers involved (Figure 4(b)). From this figure, it can again be seen that after 30m/s the proportion of consumers experiencing a fault increases significantly and that using the wind speeds in the larger DNO and Region spaces causes the vulnerability of the system to be underestimated. This is again due to the spatial differences between the location of infrastructure and the location of the wind storm.

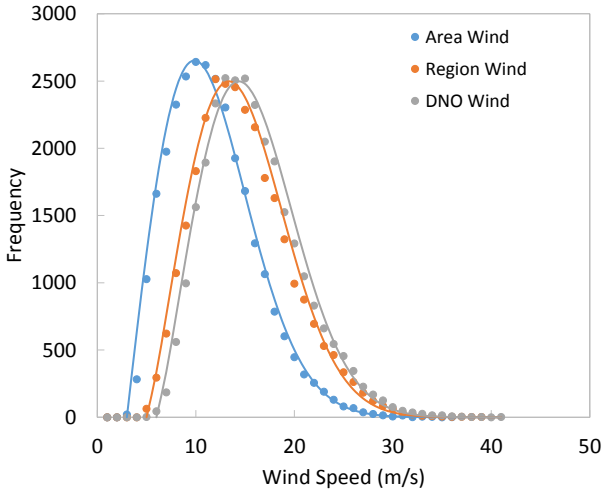

Figure 5: Plotting the number of 6 hourly intervals when each maximum wind speed value was recorded, where the wind speed has been binned to the nearest integer.

We also investigate the relationship between the number of faults and the number of consumers involved, when using the maximum wind speed in the Area space (shown in Figure 6). From this figure, it can be seen that there is a linear relationship between the two, meaning that the number of consumers involved is directly related the number of faults and that higher wind speeds causing a large number of faults are also likely to affect a large number of consumers.

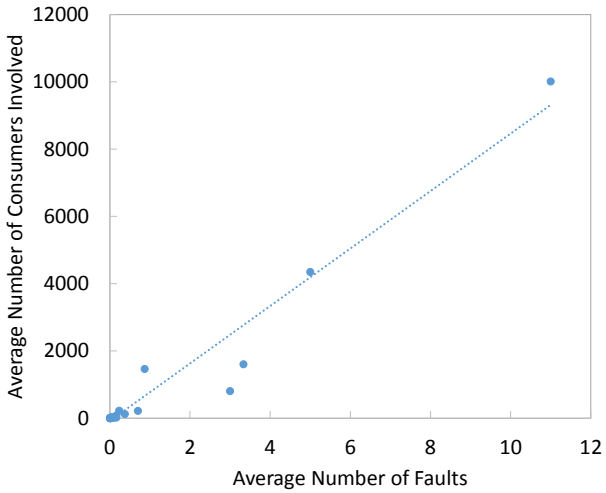

Figure 6: Plotting the average number of faults against the average number of consumers involved, when calculated using the Area wind speed.

We also consider how the coefficient of variation changes with wind speed (*Figure 7*), to give an indication of the associated uncertainty. We use this measure as it is a standardized measure of dispersion and is defined as the ratio of the standard deviation to the mean. From Figure 8, it can be seen that for both the number of faults and number of consumers affected there appears to be two distinct distributions (separated by the dashed line). The failures occurring due to low wind speeds (to the left of this line) are likely to be infrastructure components located in high risk areas (e.g. close to many trees). It can be seen that at around 12m/s there is a lower risk of potential failures occurring (indicated by the higher coefficient of variation value), but that as the wind speed increases so does the chance of at least one fault occurring on the network. At 30m/s it is almost guaranteed that there will be at least one overhead line failure on the network (indicated by the low coefficient of variation value), which will also result in a number of consumers being affected. However, it is also worth noting that there are few data points when the wind speed is over 35m/s, which may affect the results achieved. To gain a larger sample of data, future studies should consider increasing the bin size, used for the wind speed, or use data from other Areas.

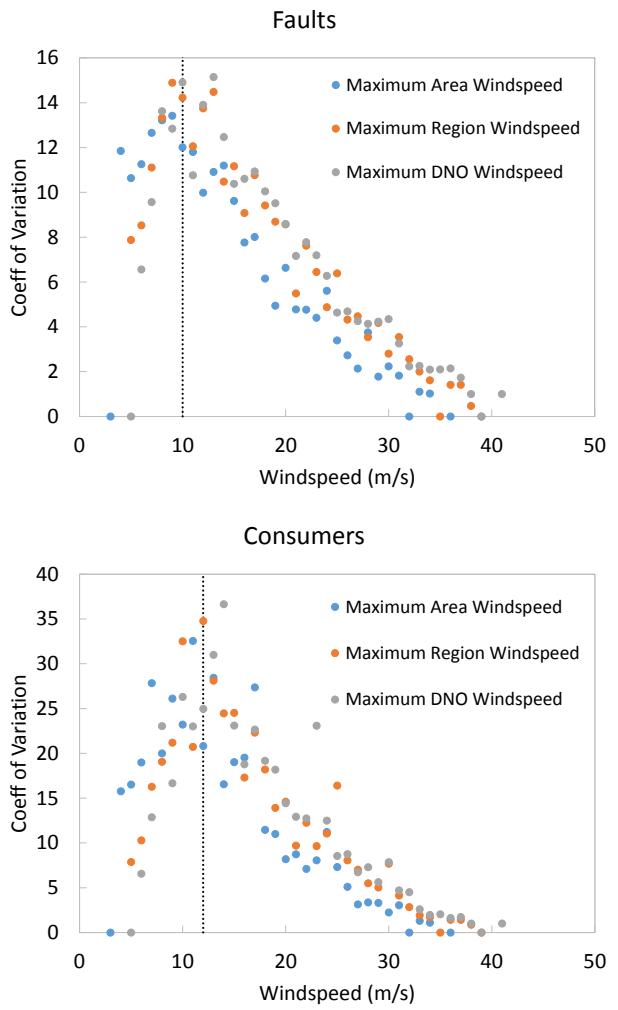

Figure 7: Plotting the coefficient of variation calculated using (a) faults and (b) consumers affected for each binned integer value of wind speed (m/s).

6. SUMMARY AND CONCLUSIONS

We have developed a series of empirical vulnerability curves for overhead line components of energy distribution infrastructure when subjected to wind storm hazards, by combining an atmospheric model with empirical fault data held in the NaFIRS database. We have also investigated the sensitivity of these vulnerability curves to the spatial resolution of wind data. The NaFIRS database records the DNO, Region and Area in which the fault occurs and therefore we have used the maximum wind speed in each of these areas to develop three vulnerability curves.

From the outputs, it can be concluded that the spatial resolution of wind data can have a significant impact to the vulnerability curve. Using a low resolution (e.g. DNO space) results in a vulnerability curve that significantly underestimates the failure wind speed of components compared to using a higher resolution of wind data (e.g. Area space) (i.e. components fail at a higher wind speed when using DNO maximum wind speeds compared to Area maximum wind speeds).

We have also investigated the coefficient of variation for the three fragility curves. From these plots it can be concluded that for low wind speeds (around 10m/s) there is a low chance of potential failures, but for wind speeds of over 30m/s there is an almost guaranteed chance of failure.

It is worth noting that in this paper we have only considered the results for one DNO in the UK, due to data restrictions. Future work should consider faults in all DNOs in the UK and the impact that this may have to the vulnerability functions.

7. ACKNOWLEDGEMENTS

We would like to acknowledge the Energy Networks Association for giving us access to the NaFIRS database and also for their insights into the management and configuration of energy distribution systems.

8. REFERENCES

Bazos, N., and Kiremidjian A. S. (1997). "Risk assessment of bridges and highway systems from the Northridge earthquake." Proceedings of the National Seismic Conference on Bridges and Highways. Sacramento, CA.

Cabinet Office (2013). "National Risk Register of Civil Emergencies." Cabinet Office. London.

Dee, D.P., Uppala, S.M., Simmons, A.J., Berrisford, P., Poli, P., Kobayashi, S., Andrae, U., Balmaseda, M.A., Balsamo, G., Bauer, P., Bechtold, P., Beljaars, A.C.M., van de Berg, L., Bidlot, J.,

Bormann, N., Delsol, C., Dragani, R., Fuentes, M., Geer, A.J., Haimberger, L., Healy, S.B., Hersbach, H., Hólm, E.V., Isaksen, L., Kållberg, P., Köhler, M., Matricardi, M., McNally, A.P., Monge-Sanz, B.M., Morcrette, J.-J., Park, B.-K., Peubey, C., de Rosnay, P., Tavolato, C., Thépaut, J.-N., and Vitart, F. (2011). "The ERA-Interim reanalysis: configuration and performance of the data assimilation system." *Quarterly Journal of the Royal Meteorological Society*, 137(656).

Ellingwood, B., Rosowsky, D., Li, Y., and Kim, J. (2004). "Fragility Assessment of Light-Frame Wood Construction Subjected to Wind and Earthquake Hazards." *Journal of Structural Engineering*, **130**(12), 1921-1930.

Energy Networks Association (2011). "Engineering Report 1: Electricity Networks Climate Change Adaptation Report".

Gittus, J. H. (2004). "Security of Supply of Electricity in the UK: Transmission and Distribution".

Grossi P., and Kunreuther H. (2005). "Catastrophe Modeling: A New Approach to Managing Risk." *New York: Springer-Verlag*.

Kaplan, S., Perla, H. F., and Bley, D. C. (1983). "A Methodology for Seismic Risk Analysis of Nuclear Power Plants." *Risk Analysis*, **3**(3), 169-180.

Kennedy, R. P., Cornell, C. A., Campbell, R. D., Kaplan, S., and Perla, H. F. (1980). "Probabilistic Seismic Safety Study of an Existing Nuclear Power Plant." *Nuclear Engineering and Design*, **59**(2), 315-338.

Lin, J. H. (2008). "Seismic fragility analysis of frame structures." *International Journal of Structural Stability and Dynamics*, **8**(3), 451-463.

McColl, L., Palin, E.J., Thornton, H.E., Sexton, D.M.H., Betts, R., and Mylne, K. (2013). "Assessing the potential impact of climate change on the UK's electricity network." *Climate Change*, **14**(1), 821-835.

Met Office (2008). "Investigating the relationship between electricity network resilience and weather. "

Pitilakis, K., Crowley, H., and Kaynia, A. (2014a). "SYNER-G: Typology Definition and Fragility Functions for Physical Elements at Seismic Risk". *Geotechnical, Geological and Earthquake Engineering*.

Pitilakis, K., Franchin, P., Khazai, B., and Wenzel, H. (2014b). "SUNER-G: Systemic Seismic Vulnerability and Risk Assesment of Complex Urban, Utility, Lifeline Systems and Critical Facilities". *Geotechnical, Geological and Earthquake Engineering.*

PricewaterhouseCoopers (2010). "Adapting to cliamte change in the infrastructure sectors."

Risk Management Solutions (2007). "The Great Storm of 1987: 20-Year Retrospective. "

Schultz, M. T., Gouldby, B. P., Simm, J. D., and Wibowo, J. L. (2010). "Beyond the Factor of Safety: Developing Fragility Curves to Characterize System Reliability." *Washington, DC, U.S. Army Corps of Engineers*.

Wilkinson, S. M., Fowler, H., Manning, L., and Dunn, S. (2014) "ECLISE Deliverable 4.07 of Task T4.5: Estimates of Extreme Wind Speed used for the Design of Buildings."

Willis Analytics (2007). "Windstorm Kyrill, 18 January 2007."